ACS OMEGA

http://pubs.acs.org/journal/acsodf

Article

Synthesis, Spectroscopic Characterization, Single-Crystal Structure, Hirshfeld Surface Analysis, and Antimicrobial Studies of 3-Acetoxy-2-methylbenzoic Anhydride

Şükriye Çakmak, Sevgi Kansiz,* Mohammad Azam,* Aysel Veyisoglu, Hasan Yakan, and Kim Min

Cite This: *ACS Omega* 2022, 7, 17192−17201

Read Online

ACCESS | Metrics & More | Article Recommendations | Supporting Information

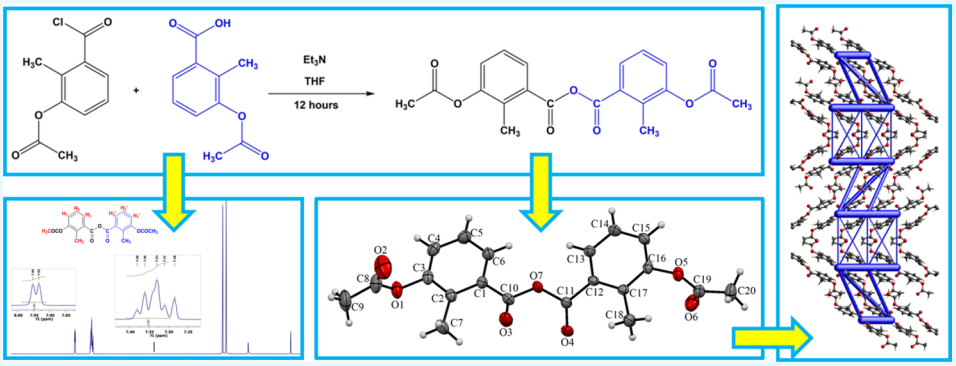

ABSTRACT: We report a novel anhydride derivative, 3-acetoxy-2-methylbenzoic anhydride (AMA), obtained from the interaction of 3-acetoxy-2-methylbenzoyl chloride with 3-acetoxy-2-methylbenzoic acid. The synthesized compound was characterized by elemental analysis, IR, ^{1}H NMR, and ^{13}C NMR spectroscopic studies and single-crystal X-ray crystallography which revealed the crystallization of AMA as monoclinic with space group $P2_1/c$. A Hirshfeld surface analysis was performed to record various intermolecular interactions, indicating the stabilization of the AMA structure by the intermolecular weak C−H···O hydrogen bonds and $\pi\cdots\pi$ interactions. The title compound was screened for antibacterial and antifungal activities using a serial dilution technique under aseptic conditions. The results indicate that the title compound has significant antibacterial properties but showed no antifungal behavior.

INTRODUCTION

The carboxylic anhydride series is a very diverse class of organic compounds that serve both as a precursor for the synthesis of esters, amides, drugs, and peptides and as a versatile reagent for numerous reactions including free carboxylic acids with alcohols, silyl esters, chemoselective esterification, lactonization, and conversion of silyl esters to lactones.[1−10] A functional group in an organic acid anhydride is highly reactive, making it rare in nature. Cantharidin, a terpene found in many species of blister beetles, is a naturally occurring anhydride of carboxylic acids.[11] Shellfish naturally contains maleic anhydride, which is produced by the bacteria *Streptomyces spiroverticillatus* in the form of the natural compound tautomycin.[12,13]

Anhydrides are compounds with two carbonyl groups attached to the same oxygen. There are many methods for synthesizing various symmetrical and unsymmetrical anhydrides in the literature.[14−16] The most common anhydrides in organic chemistry are those derived from carboxylic acids and the dehydration of carboxylic acids in the presence of dehydrating reagents like carbodiimides,[17] thionyl chlorides,[18] and isocyanates.[19] In addition, the synthesis of anhydrides has been reported by the acylation of acyl halides and anhydrides with carboxylates.[20]

Carboxylic anhydrides have been used as plasticizers for PVC and other plastics, particularly where temperature stability is required, such as in wire and cable coatings. In addition, these compounds possess a broad spectrum of antimicrobial activity.[21] Benzoic anhydride, which is added to low-density polyethylene (LDPE) during film manufacture, can control mold growth on the surface of foods such as cheese and thus have antifungal activity.[22,23] The naphthalene tetracarboxylic dianhydrides produced as precursors for the manufacture of naphthalenediimides (NDIs) have been reported to have important applications in materials science

Received: February 15, 2022
Accepted: April 26, 2022
Published: May 13, 2022

https://doi.org/10.1021/acsomega.2c00879
ACS Omega 2022, 7, 17192−17201

Scheme 1. Synthesis of the Title Compound

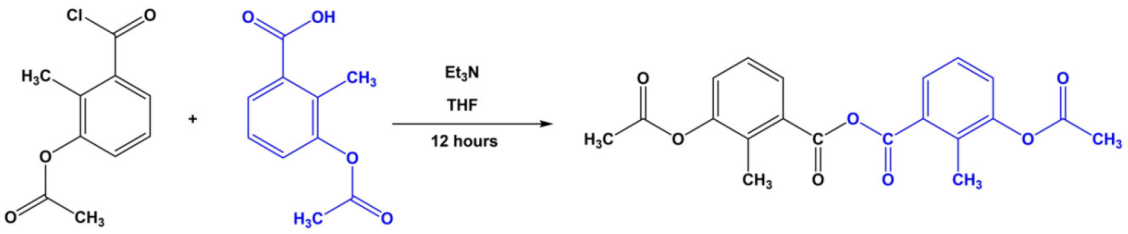

and artificial photosynthesis.[24] In the present study, we used a known and common method to synthesize the title anhydride compound. The structure of the compound was characterized using elemental analyses, IR, ^{1}H and ^{13}C NMR spectroscopy, single-crystal X-ray diffraction, and Hirshfeld surface analysis. The *in vitro* antimicrobial activity of the title anhydride was determined against six bacterial and two fungal species.

EXPERIMENTAL SECTION

Materials and Methods. The chemicals used in the experiment were procured from commercial sources and were not further purified. The solvents were of analytical grade. A Stuart SMP 30 Advanced Digital Melting Point apparatus was used to determine the melting point of the title compound. A Bruker Vertex 80 V spectrometer was used to record FT-IR spectra. Bruker/Ultraschilt spectrometers were used to record ^{1}H and ^{13}C NMR spectra. The ^{1}H spectrum was recorded at 300 MHz and the ^{13}C spectrum at 75 MHz. Elemental analyses were carried out at ODUMARAL at Ordu University using an Elementar Vario Micro Cube (Germany) elemental analyzer.

Synthesis of 3-Acetoxy-2-methylbenzoic Anhydride (AMA). Triethylamine (2.1 mL, 15 mmol) was gradually added to a solution of 3-acetoxy-2-methylbenzoic acid dissolved (15 mmol) in THF (7.5 mL), followed by the addition of 3-acetoxy-2 methylbenzoyl chloride (2.55 g, 12 mmol) dissolved in the same solvent (7.5 mL). The resultant reaction mixture was stirred at room temperature for 12 h, resulting in a white precipitate which was removed by filtration. An amount of 150 mL of deionized water was added to the resulting solution, yielding a product that was washed with deionized water to eliminate triethylamine hydrochloride. The product gives beautiful crystals when crystallized in ethanol. Scheme 1 shows a pictorial representation of the synthesis of the title compound. They were prepared with minor modifications according to a reported procedure.[25] Yield: 3.33 g, 75%; mp 118−120 °C. Anal. calcd for $C_{20}H_{18}O_7$: C, 64.86; H, 4.90. Found C, 64.90; H, 4.84.

Crystal Structure Determination. An appropriate crystal of size 0.10 × 0.06 × 0.05 mm^3 was selected to collect X-ray intensity data at 296 K (λ = 0.71073 Å) with a Bruker diffractometer equipped with Mo Kα radiation. Bruker SAINT software was used to collect rotational mode (f and ω scanning mode) reflectance measurements to compute cell parameters.[26] The integration method was used to correct for absorption (μ = 0.08 mm^{-1}). The crystal structure of the compound was solved directly using SHELXT.[27] The non-hydrogen atom positional and anisotropic temperature parameters were refined with SHELXL, using a full-matrix least-squares method, yielding 317 crystallographic parameters.[28] Anisotropic refinement of the non-hydrogen atom parameters was conducted, and a difference Fourier map was used to determine hydrogen atom positions. Various freely refined coordinates and $U_{iso}(H)$ values were applied. Using a threshold of $I > 2\sigma(I)$ to refine the structure, R_{int} = 0.0647 with 2041 reflections was observed. WinGX (version 2018.3)[29] and Mercury[30] software was used to plot numbers and obtain data in tables. Table 1 lists all the refinement details for the title compound.

Table 1. Structure Refinement Details for AMA

CCDC	2058057
chemical formula	$C_{20}H_{18}O_7$
temperature (K)	296
space group	$P2_1/c$
crystal system	monoclinic
M_r	370.34
a, b, c (Å)	6.1033 (10), 40.920 (7), 7.8767 (14)
α, β, γ (deg)	90, 111.350 (5), 90
volume, V (Å^3)	1832.2 (6)
crystal size (mm)	0.10 × 0.06 × 0.05
calculated density (Mg/m^3)	1.343
F_{000}	776
μ (mm^{-1})	0.10
Z	4
diffractometer	Bruker APEX3 CCD
θ range (deg)	$2.8 \le \theta \le 25.8$
wavelength (Å)	0.71073
measurement method	ω scan
absorption correction	multiscan
h_{min}, h_{max}	−8, 8
k_{min}, k_{max}	−54, 54
l_{min}, l_{max}	−10, 10
R_{int}	0.046
reflections collected	51787
independent reflections	4571
observed reflections [$I > 2\sigma(I)$]	2041
refinement method	SHELXL18/3
parameters	317
$R[F^2 > 2\sigma(F^2)]$	0.065
$wR(F^2)$	0.234
GooF = S	1.07
$\Delta\rho_{min}, \Delta\rho_{max}$ (e/Å^3)	−0.31, 0.31

Antimicrobial Activity. The antimicrobial activity of the title compound was evaluated in in 96-well microplates using the broth microdilution technique. The minimum inhibitory concentration (MIC) method was employed to measure the antimicrobial activity.[31−33] The pathogenic microorganisms tested are the Gram-positive strain (*Bacillus subtilis* ATCC 6633; *Staphylococcus aureus* ATCC 25923; *Enterococcus faecalis* ATCC 29212) and Gram-negative strain (*Escherichia coli* ATCC 25922; *Klebsiella pneumoniae* ATCC 70060; *Pseudomo-*

https://doi.org/10.1021/acsomega.2c00879
ACS Omega 2022, 7, 17192−17201

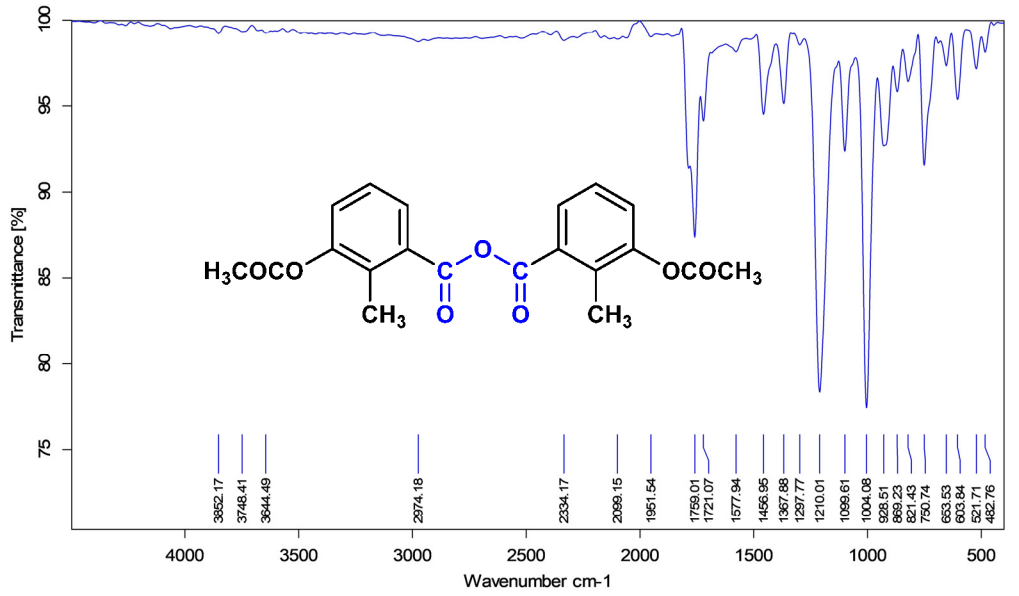

Figure 1. IR spectrum of the title compound.

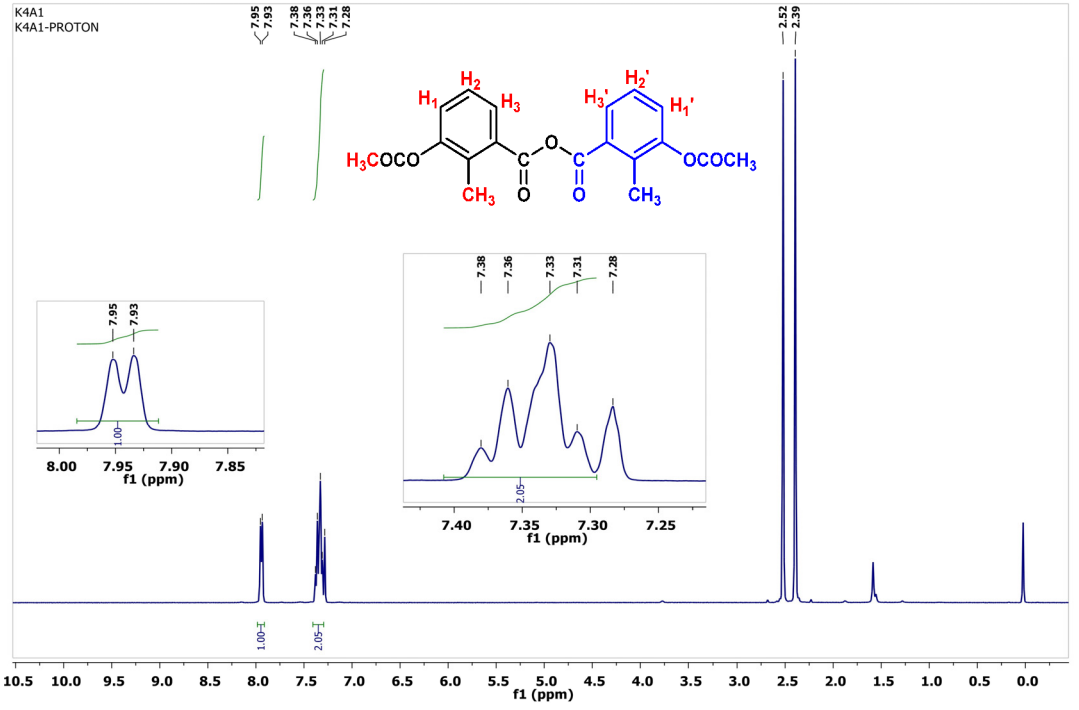

Figure 2. ^{1}H spectrum of the compound, AMA.

nas aeruginosa ATCC 27853; *Aspergillus niger* ATCC 16404; *Candida albicans* ATCC 1023). Dimethyl sulfoxide was used to dilute and dissolve the compound. The stock concentration was prepared as 2000 g/mL. All bacterial strains were cultured in broth following a 24 h incubation period at 37 °C. The fungi were incubated for 24 h at 28 °C and then kept in nutrient solution. Homogenization of bacterial and fungi cells was carried out in nutritional solution. A turbidity of approximately 10^6 cells/mL was achieved for bacterial and fungal suspensions. The only controls used were inoculated broths. The wells were filled with 100 μL each of the microorganism suspensions and 100 μL of the compound suspension to be tested. The MIC, expressed in μg/mL, was determined by recording the growth rate of microorganisms on the microtiter plate. Amoxicillin and tetracycline were used as antibacterial reference standards, with ketoconazole serving as an antifungal reference standard.

RESULTS AND DISCUSSION

Vibrational Frequencies. The C═O stretching vibrations were identified as distinguishing absorption bands at 1790 and 1759 cm^{-1} in the IR spectra. These two bands were observed as the symmetric stretching mode at the higher frequency and the asymmetric stretching mode at the lower frequency. For the −CO−O−CO− system, the symmetric stretching band is relatively weaker with the lower asymmetric stretching. The C═O stretching mode of the acetoxy groups appeared at 1721

https://doi.org/10.1021/acsomega.2c00879
ACS Omega 2022, 7, 17192−17201

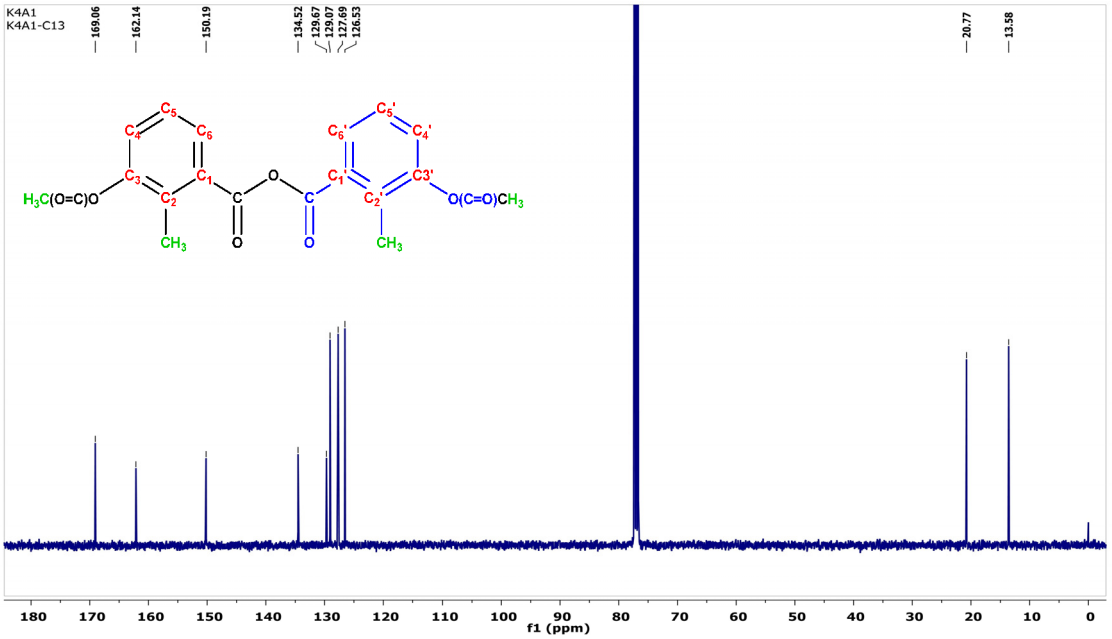

Figure 3. ^{13}C NMR spectrum of the compound.

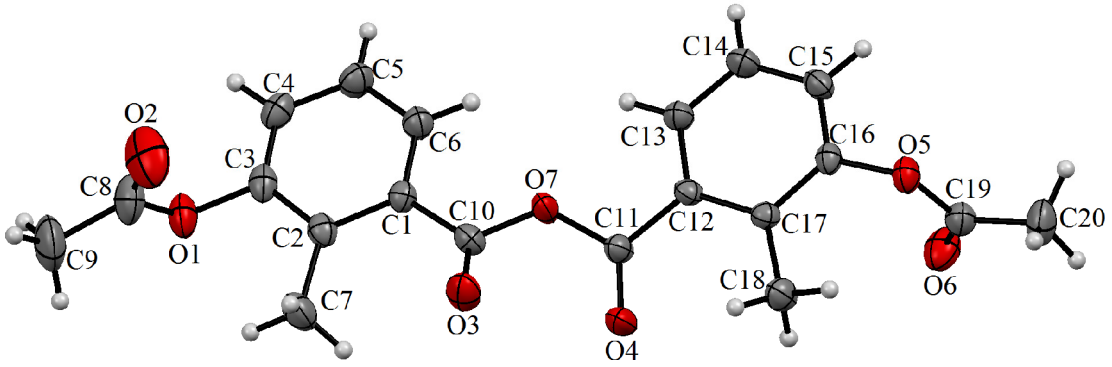

Figure 4. ORTEP diagram of the compound with atomic numbers.

cm^{-1}. The aromatic and aliphatic CH vibrations were observed at 3060−2974 and 2926−2835 cm^{-1}, respectively. The aromatic strong $\nu_{(-C-O)}$ stretch was detected at 1210 cm^{-1}, as shown in Figure 1. The stretch of the aliphatic $\nu_{(-C-O)}$ was noticed at 1004 cm^{-1}. These findings are similar to those reported previously for comparable compounds.[14,34−37]

^{1}H NMR Spectrum. The ^{1}H NMR spectrum of the title compound was measured in deuterated chloroform. A singlet of the methyl proton was observed at 2.52 ppm (s, 3H, $-OCOCH_3$) and linked to the ester carbonyl ring due to oxygen and carbonyl groups contained in the ester carbonyl group, whereas the methyl proton at the 2-position on the phenyl ring was observed at 2.39 ppm (s, 3H, Ar$-CH_3$). The protons (H1−H3) of the phenyl rings were found at 7.95−7.31 ppm in the title compound, as illustrated in Figure 2. The H1 and H2 protons, which were coupled to the H3 proton and each other, resonated as quintet peaks at 7.38−7.31 ppm (q, J = 8.0 Hz, 2H). In addition, the H1 proton is identical to the H1′ proton, and H2 and H3 protons are identical to H2′ and H3′ protons. These values appear to be consistent with values previously reported for similar compounds.[14,34,35]

^{13}C NMR Spectrum. The ^{13}C NMR spectra of the title compound, measured in $CDCl_3$, showed 10 distinct resonances that are consistent with the target compound. The carbonyl (C═O) peak of the anhydride was detected at 169.06 ppm, while the measured carbon signal due to the ester group appeared at 162.14 ppm. The C3 aromatic carbon signal occurred at 150.19 ppm. The existence of the carbonyl group on the phenyl ring causes the C1 carbon signal to move downfield and appear at 134.52 ppm. The other aromatic ring carbons ranged from 129.67 to 126.53 ppm. The C2, C4, C5, and C6 carbons were observed at 129.67, 127.69, 129.07, and 126.53 ppm, respectively. The signal at 20.77 ppm is attributed to the methyl carbon linked to the ester carbonyl group ($-OCOCH_3$), whereas the signal at 13.58 ppm is assigned to the methyl group bound phenyl ring, as illustrated in Figure 3. These values agree with previously reported values for similar compounds.[14,34,35]

Crystal Structure of AMA, $C_{20}H_{18}O_7$. The molecular structure of AMA with atom numbering is shown in Figure 4. A hydrogen atom is shown as a small sphere of arbitrary radius, and the other atoms are ellipsoids with displacement probabilities of 30%. AMA is crystallized in a monoclinic space group $P2_1/c$ with Z = 4 (Table 1). There is an independent molecule in the asymmetric unit. The title compound has nearly planar molecular geometry with a

https://doi.org/10.1021/acsomega.2c00879
ACS Omega 2022, 7, 17192−17201

Table 2. Noncovalent Interactions for AMA (Å, deg)

D−H···A	D−H	H···A	D···A	D−H···A	symmetry code
C4−H4···O2^{i}	0.93	2.59 (4)	3.424 (6)	149 (3)	(i) $x, -y + 1/2, z - 1/2$
C14−H14···O4^{ii}	0.93	2.58 (4)	3.253 (6)	130 (3)	(ii) $x - 1, y, z - 1$

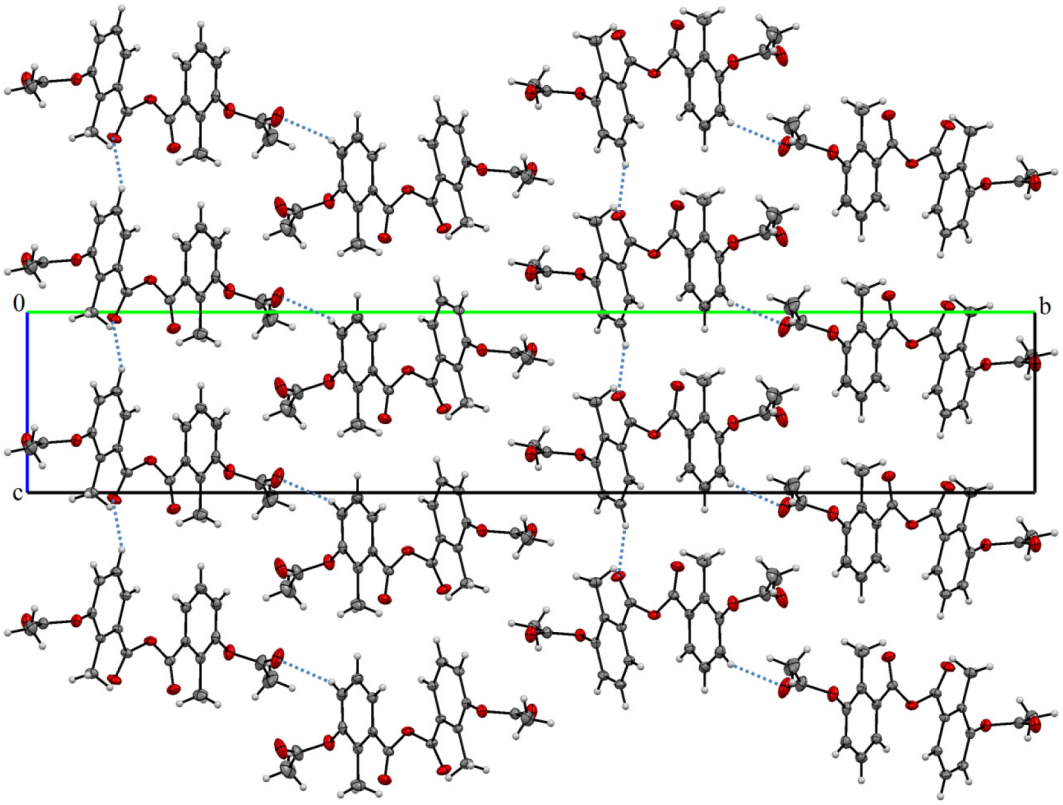

Figure 5. A view crystal packing of AMA, showing C4−H4···O2^{i} and C14−H14···O4^{ii} hydrogen bonds.

dihedral angle of 5.26° between the planes of the C1/C6 and C7/C12 six-membered aromatic rings. Noncovalent interactions such as hydrogen bonding, van der Waals interactions, and $\pi\cdots\pi$ influence the molecular conformation. Two intermolecular C−H···O bonds and two $\pi\cdots\pi$ contacts stabilize the crystalline packing of the compound in a three-dimensional network. Table 2 summarizes various contact lengths, angles, and noncovalent interactions. As illustrated in Figure 5, the intermolecular C4−H4···O2^{i} hydrogen bonds in crystal packing form a one-dimensional structure along the [101] direction, whereas the C14−H14···O4^{ii} hydrogen bond forms a chain along the [001] direction. In addition, the $\pi\cdots\pi$ interactions shown in Figure 6 also generate a chain motif along [100]. These weak $\pi\cdots\pi$ interactions are $Cg1\cdots Cg2$ ($x + 1, y, z$) = 3.8453 (7) Å and $Cg2\cdots Cg1$ ($x-1, y, z$) = 3.8453 (7) Å; $Cg1$ and $Cg2$ are the centroids of the C1−C6 and C7−C12 rings, respectively. The arrangements of O3 = C10−O7 and O4 = C11−O7 groups are not planar with respect to their carrier benzene rings (C1/C6 and C7/C12), with dihedral angles of 15.8(4)° and 19.3(30)°, respectively. The central anhydride moieties C1−C10−O3−O7 and C12−C11−O4−O7 are twisted with a dihedral angle of 34.8(2)°. The torsion angles of O3−C10−O7−C11, O4−C11−O7−C10, C2−C1−C10−O3, and C17−C12−C11−O4 are 19.7(5)°, 23.1(5)°, −17.2(5)°, and −20.1(5)°, respectively. It is clearly seen that the central anhydride group is not planar with these angle values. C−O double bond lengths are in the range of 1.184−1.199 Å. Some selected bong lengths and angles are given in Table 3. When compared with the recently reported phthalic anhydride containing studies, C−O double bond lengths appear to be in agreement with the values in this study.[38,39]

Hirshfeld Surface Analyses. The Hirshfeld surface was analyzed with CrystalExplorer21 to identify various intermolecular contacts in the crystal structure.[40−46] The analysis of the 3D Hirshfeld surface (HS) and 2D fingerprint plots (FPs) were performed in order to describe the molecular structure of AMA. The surfaces mapped over d_{norm}, shape index, and curvedness were shown in Figure 7. Complementary pairs of triangles are seen on both surfaces of the molecule, for the shape index surface, indicating that the respective π-stacking interactions are present in the crystal packing for the title compound. In Figure 7, the $\pi\cdots\pi$ interactions for the compound correspond to the relatively large green flat regions on the curvedness surfaces and are evident on both sides of the rotated molecule. Like the title compound, in the 1-acylthiourea derivative recently reported, namely, 1-(2-oxo-2*H*-chromene-3-carbonyl)-3-(2-methoxyphenyl)thiourea, the molecule is linked by the $\pi\cdots\pi$ interactions.[47] Similarly, the shape index surface has a connecting complementary pair of triangles, and the curvedness surface has large green flat regions. This means that the corresponding π-stacking interactions are present in the crystal packing for the given structure. The 3D d_{norm} surface is mapped to a fixed color scale from −0.1183 to 1.3829 Å, showing that the largest contribution to crystal

https://doi.org/10.1021/acsomega.2c00879
ACS Omega 2022, 7, 17192−17201

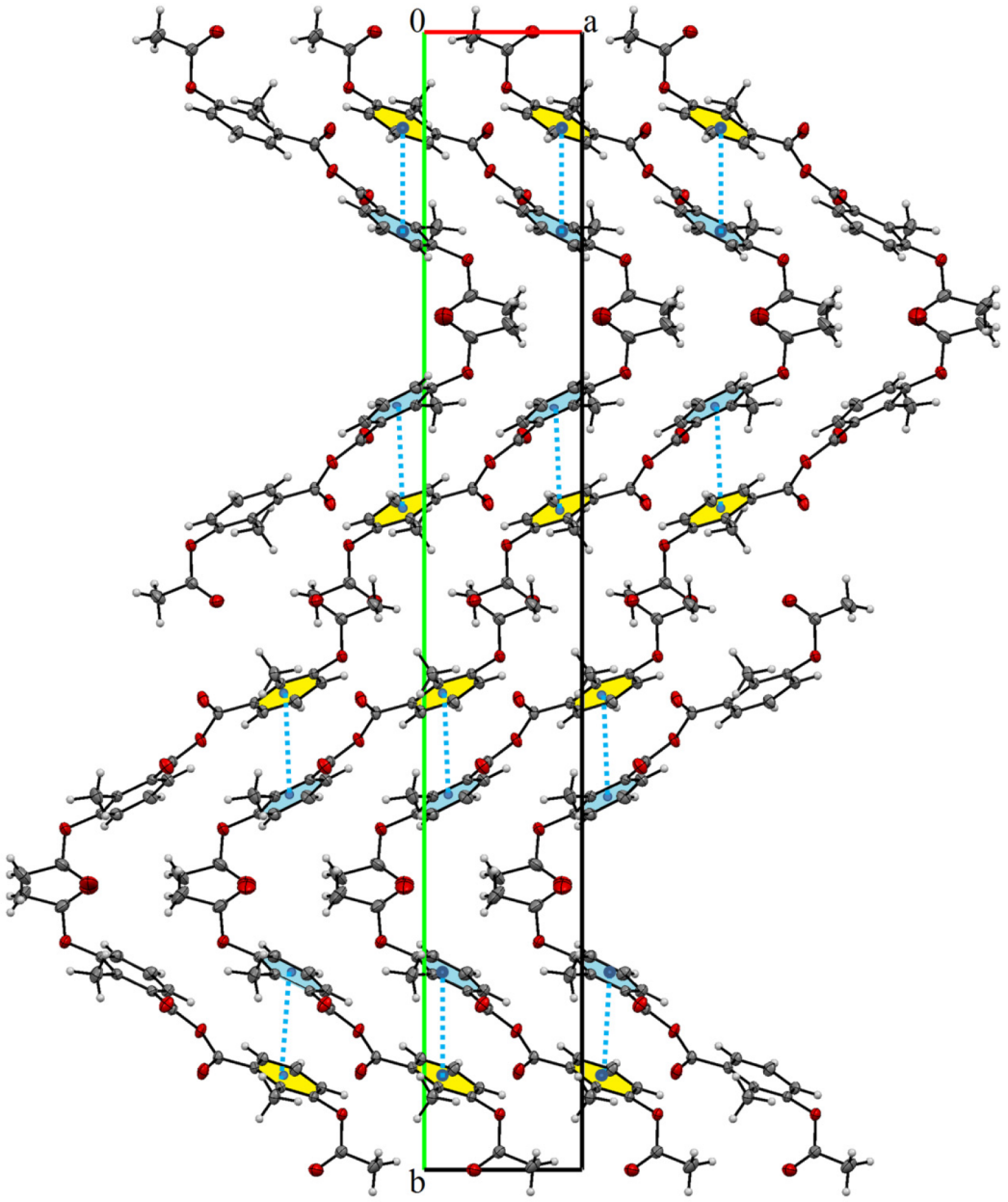

Figure 6. Π···π interactions in AMA shown along the [100] axis.

Table 3. Selected Geometric Parameters of AMA (Å, deg)

geometric parameters		geometric parameters	
bond lengths (Å)	X-ray	bond angles (deg)	X-ray
C8−O1	1.349 (5)	O1−C8−O2	121.7 (4)
C3−O1	1.411 (4)	O7−C10−O3	121.6 (3)
C8−O2	1.184 (5)	O7−C11−O4	121.4 (3)
C10−O3	1.199 (4)	O5−C19−O6	122.0 (3)
C11−O4	1.195 (3)	C3−O1−C8	118.3 (3)
C16−O5	1.409 (3)	C16−O5−C19	118.1 (2)
C19−O5	1.357 (4)	C1−C10−O7	111.1 (3)
C19−O6	1.196 (4)	C12−C11−O7	111.2 (3)
C10−O7	1.381 (4)	torsion angles (deg)	
C11−O7	1.393 (4)	C1−C2−C3−O1	176.4 (3)
C2−C7	1.509 (5)	C14−C15−C16−O5	−176.3 (3)
C8−C9	1.499 (6)	C2−C1−C10−O7	165.9 (3)
C19−C20	1.485 (5)	C17−C12−C11−O7	164.3 (3)

packing comes from interactions between H atoms, covering a significant region of the entire HS (45.5%). Figure 8 shows the fingerprint plots with two symmetrical peaks associated with O···H interactions (29.5%), correlating with intermolecular hydrogen bonds between C4−H4···O2^{i} and C14−H14···O4^{ii}. The asymmetric contact wings of C···H with a relative contribution of 12.4% can be seen on both sides of the relevant plots. C···O (6.2%), C···C (4.4%), and O···O (2%) are the less important interactions.

Energy framework analysis was performed by CrystalExplorer21 to obtain the intermolecular interaction energies, allowing analysis and visualization of the three-dimensional crystal packing to analyze and visualize the three-dimensional crystal topology. The interaction energy is calculated using the formula $E_{tot} = E_{ele} + E_{pol} + E_{dis} + E_{rep}$ (where E_{ele} is the electrostatic component, E_{pol} the polarization energy, E_{dis} the dispersion energy, and E_{rep} the exchange repulsion energy). The energy framework is depicted in Figure 8. Clusters of 3.8

https://doi.org/10.1021/acsomega.2c00879
ACS Omega 2022, 7, 17192−17201

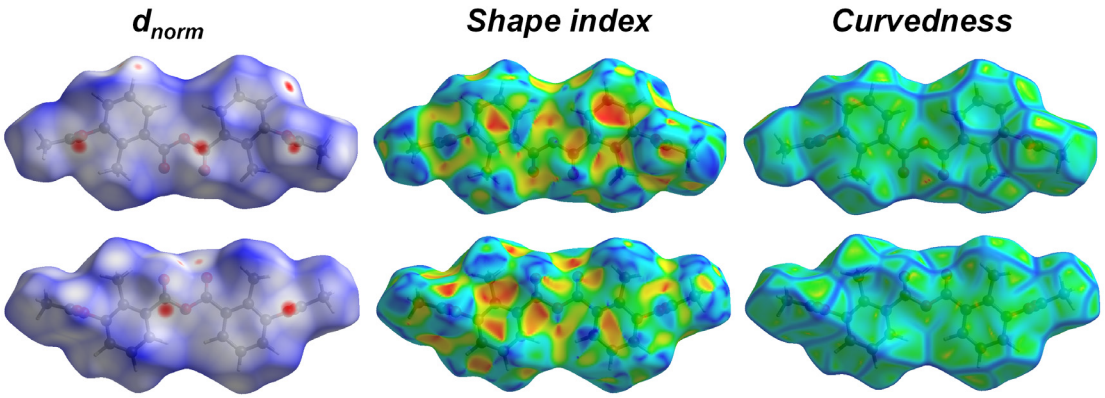

Figure 7. Hirshfeld surfaces d_{norm}, shape index, and curvedness for AMA. Molecule is shown in two orientations.

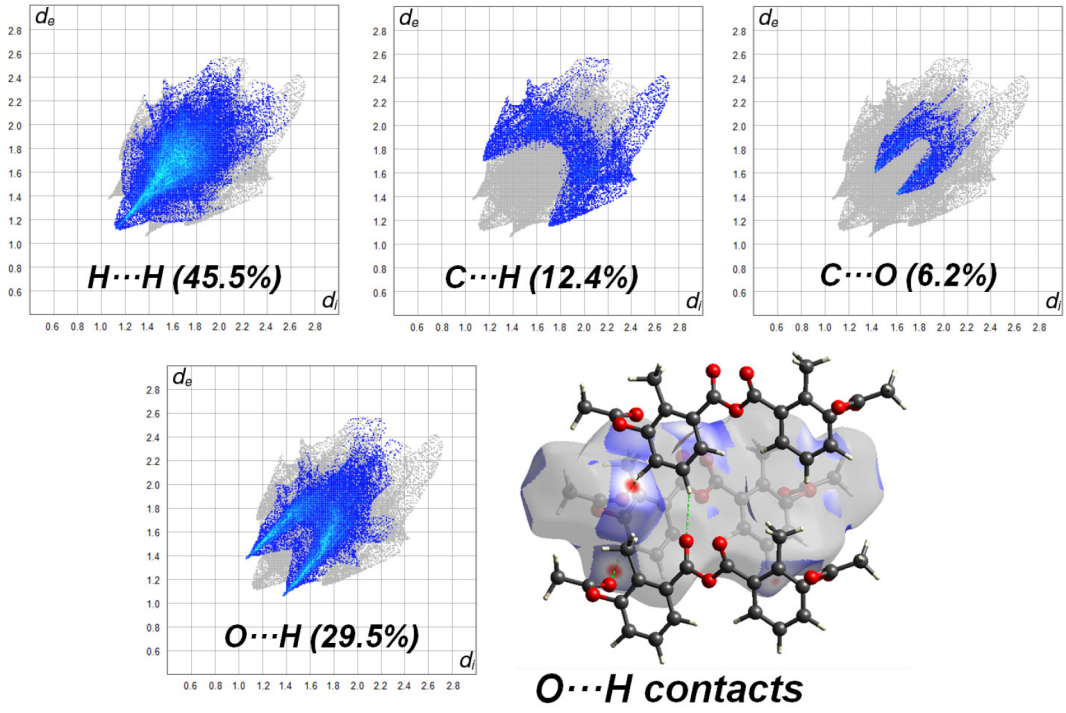

Figure 8. Two-dimensional fingerprint plots and HS for AMA.

Å were formed around each molecule. The tube size used was 100 with a cutoff value of 5 kJ/mol. The thickness of the tube in Figure 9 is proportional to the values of the interaction energies. The total interaction energies are repulsion (E_{rep} = 42.1 kJ/mol), dispersion (E_{dis} = −160.1 kJ/mol), polarization (E_{pol} = −21.6 kJ/mol), electrostatics (E_{ele} = −70 kJ/mol), and total interaction energy (E_{tot} = −209.6 kJ/mol). The dispersion component contributed 63% and the electrostatic component 28% to lattice stabilization. The 9% contribution belongs to the polarization and repulsion energies. For the compound, the sum of dispersion energies (−160 kJ/mol) is greater than that of electrostatic energies (−70 kJ/mol). According to the result obtained from these calculated values, the superiority of the dispersion energy framework over the electrostatic energy framework is clearly seen. In this study, the dispersion energies have a significant contribution in agreement with reported values.[48,49]

Antimicrobial Activity. The *in vitro* antimicrobial activity of the anhydride compound was evaluated against Gram-strain positive and negative bacterial strains, as well as two fungal strains. The MIC values were evaluated against Gram-positive and Gram-negative bacteria at doses of 500−1000 μg/mL. The tested compound exhibited excellent antibacterial activity against *S. aureus* and *E. faecalis* in comparison to standard amoxicillin, and it was also equally effective against *K. pneumoniae* and *P. aeruginosa*. In addition, the title anhydride showed less activity against *B. subtilis* and *E. coli* than standards and showed no activity against fungi. The antimicrobial activity of the title anhydride is given in Table 4.

CONCLUSIONS

A novel 3-acetoxy-2-methylbenzoic anhydride compound was investigated by elemental analysis, FT-IR, ^{1}H and ^{13}C NMR spectroscopy, and single-crystal X-ray crystallography. The X-ray findings show that a molecule has a nearly planar shape with an angle of 5.26° between the planes of the six-membered aromatic rings. There are different types of noncovalent interactions involved in creating the 3D network of the compound. The Hirshfeld surface analysis findings suggest that the H···H (45.5%), O···H (29.5%), and C···H (12.4%)

https://doi.org/10.1021/acsomega.2c00879
ACS Omega 2022, 7, 17192−17201

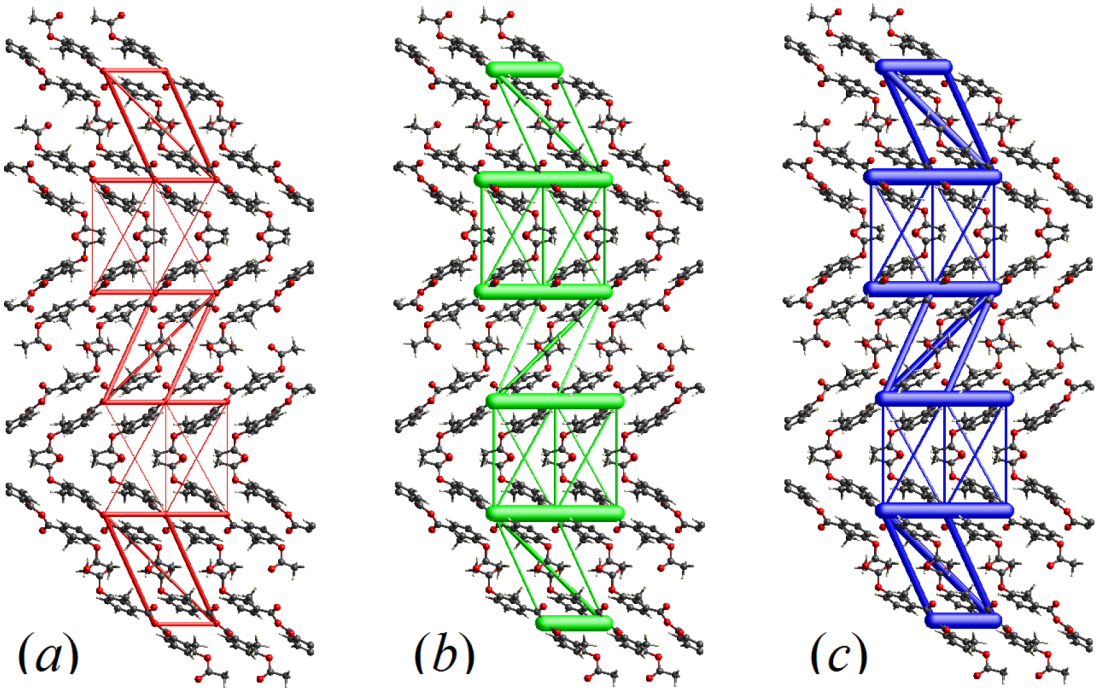

Figure 9. Energy framework diagram for (a) electrostatic (red), (b) dispersion (green), and (c) total interaction energy (blue) of AMA.

Table 4. Minimum Inhibitory Concentrations (MICs) of the AMA Compound[a]

	minimum inhibition concentration (μg/mL)							
	Gram-straining-positive			Gram-straining-negative			Fungi	
sample	*B. subtilis*	*S. aureus*	*E. faecalis*	*E. coli*	*K. pneumoniae*	*P. aeruginosa*	*A. niger*	*C. albicans*
3-acetoxy-2-methylbenzoic anhydride	1000	500	500	1000	1000	1000	-	-
amoxicillin	<2	>1000	>1000	32	>1000	>1000	NT	NT
tetracycline	<2	8	8	<2	8	4	NT	NT
ketoconazole	NT	NT	NT	NT	NT	NT	1	2

[a]NT: not tested.

interactions contribute the most to crystal packing. Although the topologies of E_{dis} and E_{ele} are similar in the title compound, the dispersion energy framework makes a larger contribution to the total energy framework. When compared to the amoxicillin standard, AMA demonstrated remarkable antibacterial activity against the Gram-positive strains *S. aureus* and *E. faecalis*, as well as being equally efficient against the Gram-negative strains *K. pneumoniae* and *P. aeruginosa*. However, it showed less antimicrobial activity than standard antibiotics in the Gram-positive *B. subtilis* strain and in the Gram-negative *E. coli* strain but not in fungi.

■ ASSOCIATED CONTENT

Supporting Information

The Supporting Information is available free of charge at https://pubs.acs.org/doi/10.1021/acsomega.2c00879.

CCDC 2058057 contains all of the crystallographic data and is freely available at www.ccdc.cam.ac.uk/structures (CIF)

■ AUTHOR INFORMATION

Corresponding Authors

Sevgi Kansiz − *Department of Fundamental Sciences, Faculty of Engineering, Samsun University, Samsun 55420, Turkey*; Email: sevgi.kansiz@samsun.edu.tr

Mohammad Azam − *Department of Chemistry, College of Science, King Saud University, Riyadh 11451, Saudi Arabia*; orcid.org/0000-0002-4274-2796; Email: azam_res@yahoo.com

Authors

Şükriye Çakmak − *Department of Medical Services and Techniques, Vocational School of Health Services, Sinop University, 57000 Sinop, Turkey*

Aysel Veyisoglu − *Department of Medical Services and Techniques, Vocational School of Health Services, Sinop University, 57000 Sinop, Turkey*

Hasan Yakan − *Department of Science and Mathematics Education, Ondokuz Mayıs University, Samsun 55139, Turkey*

Kim Min − *Department of Safety Engineering, Dongguk University, Gyeongju 780714 Gyeongbuk, South Korea*

Complete contact information is available at: https://pubs.acs.org/10.1021/acsomega.2c00879

Notes

The authors declare no competing financial interest.

https://doi.org/10.1021/acsomega.2c00879
ACS Omega 2022, 7, 17192−17201

■ ACKNOWLEDGMENTS

The authors acknowledge the financial support through Researchers Supporting Project number (RSP-2021/147), King Saud University, Riyadh, Saudi Arabia.

■ REFERENCES

(1) Ogliaruso, M. A.; Wolfe, J. F. *Synthesis of carboxylic acids, esters, and their derivatives*; Wiley: New York, NY, 1991; p 198.
(2) Tarbell, D. S. Carboxylic carbonic anhydrides and related compounds. *Acc. Chem. Res.* **1969**, *2*, 296−300.
(3) Held, H.; Rengstl, A.; Mayer, D. *Acetic anhydride and mixed fatty acid anhydrides, Ullmann's Encyclopedia of Industrial Chemistry*; Wiley-VCH: Weinheim, Germany, 2002.
(4) Rebek, J.; Feitler, D. Mechanism of the carbodiimide reaction. II. Peptide synthesis on the solid phase. *J. Am. Chem. Soc.* **1974**, *96*, 1606−1607.
(5) Kocz, R.; Roestamadji, J.; Mobashery, S. A convenient triphosgene-mediated synthesis of symmetric carboxylic acid anhydrides. *J. Org. Chem.* **1994**, *59*, 2913−2914.
(6) Kazemi, F.; Sharghi, H.; Nasseri, M. A. A Cheap, Simple and efficient method for the preparation of symmetrical carboxylic acid anhydrides. *Synthesis* **2004**, 205−207.
(7) Kazemi, F.; Kiasat, A. R.; Mombaini, B. Simple preparation of symmetrical Carboxylic acid anhydrides by means of Na_2CO_3/$SOCl_2$. *Synth. Commun.* **2007**, *37*, 3219−3223.
(8) Kawamura, Y.; Sato, Y.; Horie, T.; Tsukayama, M. Dehydration induced by intramolecular redox character of a stable allylidene-tributylphosphorane. *Tetrahedron Lett.* **1997**, *38*, 7893−7896.
(9) Keshavamurthy, S.; Vankar, Y. D.; Dhar, D. N. Preparation of acid anhydrides, amides, and esters using chlorosulfonyl isocyanate as a dehydrating agent. *Synthesis* **1982**, *1982*, 506−508.
(10) Clarke, P. A.; Kayaleh, N. E.; Smith, M. A.; Baker, J. R.; Bird, S. J.; Chan, C. A one-step procedure for the monoacylation of symmetrical 1,2-diols. *J. Org. Chem.* **2002**, *67*, 5226−5231.
(11) Epstein, W. L.; Kligman, A. M. Treatment of warts with cantharidin. *AMA Arch. Derm.* **1958**, *77*, 508−511.
(12) Oikawa, M.; Ueno, T.; Oikawa, H.; Ichihara, A. Total synthesis of tautomycin. *J. Org. Chem.* **1995**, *60*, 5048−5068.
(13) Cheng, X.-C.; Kihara, T.; Kusakabe, H.; Magae, J.; Kobayashi, Y.; Fang, R.-P.; Ni, Z.-F.; Shen, Y.-C.; Yamaguchi, I.; Isono, K. A new antibiotic, tautomycin. *J. Antibiot. (Tokyo)* **1987**, *40*, 907−909.
(14) Khatun, N.; Santra, S. K.; Banerjee, A.; Patel, B. K. Nano CuO catalyzed cross dehydrogenative coupling (CDC) of aldehydes to anhydrides. *Eur. J. Org. Chem.* **2015**, *2015*, 1309−1313.
(15) Adib, M.; Rajai-Daryasarei, S.; Pashazadeh, R.; Tajik, M.; Mirzaei, P. Regioselective transition metal-free acylation of coumarins via cross-dehydrogenative coupling reaction of coumarins and aldehydes. *Tetrahedron Lett.* **2016**, *57*, 3701−3705.
(16) Nuree, Y.; Singha, R.; Ghosh, M.; Roy, P.; Ray, J. K. Cu (I) catalyzed synthesis of anhydrides from aldehydes via CDC-pathway at ambient temperature. *Tetrahedron Lett.* **2016**, *57*, 1479−1482.
(17) Hata, T.; Tajima, K.; Mukaiyama, T. A convenient method for the preparation of acid anhydrides from metallic carboxylates. *Bull. Chem. Soc. Jpn.* **1968**, *41* (11), 2746−2747.
(18) Kazemi, F.; Kiasat, A. R. Dabco/$SOCl_2$, mild, and convenient reagent for the preparation of symmetrical carboxylic acid anhydrides. *Phosphorus Sulfur Silicon Relat. Elem.* **2003**, *178* (10), 2287−2291.
(19) Olah, G. A.; Vankar, Y. D.; Arvanaghi, M.; Sommer, J. Formic anhydride. *Angew. Chem., Int. Ed. Engl.* **1979**, *18* (8), 614−614.
(20) Rambacher, P.; Mäke, S. Simplified process for preparation of anhydrides of aromatic acids. *Angew. Chem., Int. Ed. Engl.* **1968**, 7 (6), 465−465.
(21) Ogliaruso, M. A.; Wolfe, J. F. In *Acid Derivatives (1979) Supplement B: Part 1*; Patai, S., Ed.; Wiley: New York, 1979; Vol. *1*, p 267.
(22) Chen, X.; Zheng, Y.; Shen, Y. Natural products with maleic anhydride structure: Nonadrides, tautomycin, chaetomellic anhydride, and other compounds. *Chem. Rev.* **2007**, *107*, 1777−1830.
(23) Weng, Y. M.; Hotchkiss, J. H. Anhydrides as antimycotic agents added to polyethylene films for food packaging. *Packag. Technol. Sci.* **1993**, *6*, 123−128.
(24) Bhosale, S. V.; Jani, C. H.; Langford, S. J. Chemistry of naphthalene diimides. *Chem. Soc. Rev.* **2008**, *37*, 331−342.
(25) Kawanami, Y.; Dainobu, Y.; Inanaga, J.; Katsuki, T.; Yamaguchi, M. Synthesis of thiol esters by carboxylic trichlorobenzoic anhydrides. *Bull. Chem. Soc. Jpn.* **1981**, *54* (3), 943−944.
(26) *APEX2*; Bruker AXS Inc.: Madison WI, 2013.
(27) Sheldrick, G. M. Crystal structure refinement with SHELXL. *Acta Crystallogr. C: Struct. Chem.* **2015**, *71*, 3−8.
(28) Sheldrick, G. M. SHELXT-Integrated space-group and crystal-structure determination. *Acta Crystallogr. A: Found. Adv.* **2015**, *71*, 3−8.
(29) Farrugia, L. J. WinGX and ORTEP for Windows: an update. *J. Appl. Crystallogr.* **2012**, *45*, 849−854.
(30) Macrae, C. F.; Bruno, I. J.; Chisholm, J. A.; Edgington, P. R.; McCabe, P.; Pidcock, E.; Rodriguez-Monge, L.; Taylor, R.; van de Streek, J.; Wood, P. A. Mercury CSD 2.0-new features for the visualization and investigation of crystal structures. *J. Appl. Crystallogr.* **2008**, *41*, 466−470.
(31) Sarker, S. D.; Nahar, L.; Kumarasamy, Y. Microtitre plate-based antibacterial assay incorporating resazurin as an indicator of cell growth, and its application in the in vitro antibacterial screening of phytochemicals. *Methods* **2007**, *42*, 321−324.
(32) Wayne, P. National committee for clinical laboratory standards. *Performance standards for antimicrobial disc susceptibility testing* **2002**, *12*, 01−53.
(33) Wiegand, I.; Hilpert, K.; Hancock, R. E. Agar and broth dilution methods to determine the minimal inhibitory concentration (MIC) of antimicrobial substances. *Nat. Protoc.* **2008**, *3*, 163−175.
(34) Li, Y.; Xue, D.; Wang, C.; Liu, Z.-T.; Xiao, J. Carboxylic acid anhydrides via Pd-catalyzed carbonylation of aryl halides at atmospheric CO pressure. *Chem. Commun.* **2012**, *48*, 1320−1322.
(35) Saberi, D.; Shojaeyan, F.; Niknam, K. Oxidative self-coupling of aldehydes in the presence of CuCl2/TBHP system: direct access to symmetrical anhydrides. *Tetrahedron Lett.* **2016**, *57*, 566−569.
(36) Nakamoto, K. *Infrared Spectra of Inorganic and Coordination Compounds*; Wiley Interscience: New York, 1970; p 317.
(37) Nyquist, R. A. Interpreting infrared, Raman, and nuclear magnetic resonance spectra. *Chapter 11 - Anhydrides*; Academic Press, 2001; Vol. *1*, pp 205−212.
(38) Fatima, A.; Khanum, G.; Sharma, A.; Garima, K.; Savita, S.; Verma, I.; Siddiqui, N.; Javed, S. Computational, spectroscopic, Hirshfeld surface, electronic state and molecular docking studies on phthalic anhydride. *J. Mol. Struct.* **2022**, *1249*, 131571.
(39) Dardeer, H. M.; Mahgoub, M. Y.; da Silva, J. F.; Elboray, E. E. Synthesis, crystal structure and supramolecular analysis of chlorendic acid derivatives. *J. Mol. Struct.* **2021**, *1228*, 129458.
(40) Spackman, P. R.; et al. CrystalExplorer: A program for Hirshfeld surface analysis, visualization and quantitative analysis of molecular crystals. *J. Appl. Cryst.* **2021**, *54*, 1006−1011.
(41) Spackman, M. A.; Byrom, P. G. A novel definition of a molecule in a crystal. *Chem. Phys. Lett.* **1997**, *267*, 215−220.
(42) Ashfaq, M.; Tahir, M. N.; Muhammad, S.; Munawar, K. S.; Ali, A.; Bogdanov, G.; Alarfaji, S. S. Single-crystal investigation, Hirshfeld surface analysis, and DFT study of third-order NLO properties of unsymmetrical acyl thiourea derivatives. *ACS Omega* **2021**, *6*, 31211−31225.
(43) Demircioglu, Z.; Kastas, C. A.; Kastas, G.; Ersanlı, C. C. Synthesis, crystal structure, computational chemistry studies and Hirshfeld surface analysis of two Schiff bases, (E)-2-[(4-bromo-2-methylphenylimino)methyl]-4-methylphenol and (E)-2-[(4-bromo-2-methylphenylimino)methyl]-6-methylphenol. *Molecular Crystals and Liquid Crystals* **2021**, *723* (1), 45−61.
(44) Al-Thamili, D. M.; Almansour, A. I.; Arumugam, N.; Kansız, S.; Dege, N.; Soliman, S. M.; Azam, M.; Kumar, R. S. Highly functionalized N-1-(2-pyridinylmethyl)-3,5-bis[(E)-arylmethylidene]-

https://doi.org/10.1021/acsomega.2c00879
ACS Omega 2022, 7, 17192−17201

tetrahydro-4(1H)-pyridinones: Synthesis, characterization, crystal structure and DFT studies. *J. Mol. Struct.* **2020**, *1222*, 128940.
(45) Boshaala, A.; Abrahem, A. F.; Almughery, A. A.; Al-Zaqri, N.; Zorrouk, A.; Lgaz, H.; Warad, I. Spectroscopic insight into tetrahedrally distorted square planar copper(II) complex: XRD/HSA, physicochemical, DFT, and thermal investigations. *Crystals* **2021**, *11*, 1179.
(46) Çakmak, Ş.; Koşar Kırca, B.; Veyisoglu, A.; Yakan, H.; Ersanlı, C. C.; Kütük, H. Experimental and theoretical investigations on a furan-2-carboxamide-bearing thiazole: synthesis, molecular characterization by IR/NMR/XRD, electronic characterization by DFT, Hirshfeld surface analysis and biological activity. *Acta Crystallogr. Section C: Struct. Chem.* **2022**, *78* (3), 201−211.
(47) Saeed, A.; Ashraf, S.; Florke, U.; Delgado Espinoza, Z. Y.; Erben, M. F.; Perez, H. Supramolecular self-assembly of a coumarine-based acylthiourea synthon directed by π-stacking interactions: Crystal structure and Hirshfeld surface analysis. *J. Mol. Struct.* **2016**, *1111*, 76−83.
(48) Saeed, A.; Floerke, U.; Fantoni, A.; Khurshid, A.; Pérez, H.; Erben, M. F. F. A close insight into the nature of intermolecular interactions in dihydropyrimidine-2(*1H*)-thione derivatives. *CrystEngComm* **2017**, *19*, 1495−1508.
(49) Saeed, A.; Khurshid, A.; Floerke, U.; Echeverria, G. A.; Piro, O. E.; Gil, D. M.; Rocha, M.; Frontera, A.; Mumtaz, A.; El-Seedi, H.; Erben, M. F. F. Intermolecular interactions in antipyrine-like derivatives 2-halo-*N*-(1,5-dimethyl-3-oxo-2-phenyl-2,3-dihydro-1-*H*-pyrazol-4-yl)benzamides: X-ray structure, Hirshfeld surface analysis and DFT calculations. *New J. Chem.* **2020**, *44*, 19541−19554.

https://doi.org/10.1021/acsomega.2c00879
ACS Omega 2022, 7, 17192−17201